analytical chemistry

Article

pubs.acs.org/ac

Host–Guest Interaction of Adamantine with a β-Cyclodextrin-Functionalized AuPd Bimetallic Nanoprobe for Ultrasensitive Electrochemical Immunoassay of Small Molecules

Lisong Wang, Jianping Lei,* Rongna Ma, and Huangxian Ju*

State Key Laboratory of Analytical Chemistry for Life Science, School of Chemistry and Chemical Engineering, Nanjing University, Nanjing 210093, P. R. China

Supporting Information

ABSTRACT: A modular labeling strategy was presented for electrochemical immunoassay via supramolecular host–guest interaction between β-cyclodextrin (β-CD) and adamantine (ADA). An ADA-labeled antibody (ADA–Ab) was synthesized via amidation, and the number of ADA moieties loaded on a single antibody was calculated to be ~7. The β-CD-functionalized gold–palladium bimetallic nanoparticles (AuPd–CD) were synthesized in aqueous solution via metal-S chemistry and characterized with transmission electron microscopy and X-ray photoelectron spectra. After the ADA–Ab was bound to the antigen-modified electrode surface with a competitive immunoreaction, AuPd–CD as a signal tag was immobilized onto the immunosensor by a host–guest interaction, leading to a large loading of AuPd nanoparticles. The highly efficient electrocatalysis by AuPd nanoparticles for $NaBH_4$ oxidation produced an ultrasensitive response to chloramphenicol as a model of a small molecule antigen. The immunoassay method showed a wide linear range from 50 pg/mL to 50 μg/mL and a detection limit of 4.6 pg/mL. The specific recognition of antigen by antibody resulted in good selectivity for the proposed method. The host–guest interaction strategy provided a universal labeling approach for the ultrasensitive detection of small molecule targets.

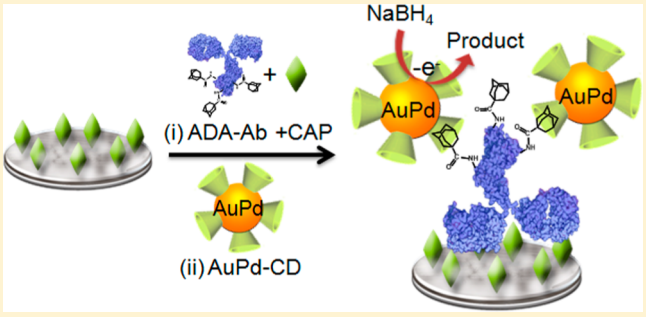

Immunoassay as a specific and sensitive method has been extensively used in clinical diagnosis,[1−6] environmental protection,[7,8] and food safety.[9,10] Owing to the space limitation of a small molecule target, the competitive approach is generally adopted for enhancing the signal readout by coupling with an enzyme- or nanoparticle-labeled antibody.[11−13] For example, horseradish peroxidase-labeled microcystin-LR antibody has been used for electrochemical detection of microcystin-LR at a microcystin-LR/carbon nanohorn-modified electrode surface.[11] However, for achieving efficient competitive binding to the immobilized antigen and the target in solution, the antibody is usually labeled with a small tag, which provides a low amount of label for each binding event and thus leads to low sensitivity and a limited detection range. To achieve signal amplification and improve the analytical performance of the competitive immunoassay, this work used a small molecule, adamantine (ADA), as a guest to label the antibody, and a multilabel detection platform was designed via supramolecular chemistry.

Supramolecular host–guest recognition via noncovalent interaction is a significant method for the assembly of large functional structures.[14,15] Because the recognition motifs are specific and bioorthogonal without an additional catalyst,[16] the host–guest interaction has been extensively applied in bioanalysis.[17−22] For example, supramolecular multivalent assembly of β-cyclodextrin (β-CD)-decorated gold nanoparticles with ferrocene dimer has been used for ultrasensitive optical enzyme sensing,[23] and a fluorescence immunoassay method has been proposed for the host–guest interaction between β-CD and ADA for detection of cellular biomarkers.[24] On the basis of construction simplicity, feasible miniaturization, and high sensitivity of the electrochemical technique, we synthesized β-CD-functionalized gold–palladium (AuPd) bimetallic nanoparticles to combine the host–guest interaction of β-CD with ADA guest-labeled antibody and the high catalytic activity of AuPd nanoparticles. The small-molecule label not only made the competitive binding more efficient but also increased the amount labeled on a single antibody for further binding of the signal tag by the host–guest interaction.

Palladium-based nanoparticles are highly efficient catalysts to facilitate the reaction of both oxygen reduction and hydrogen oxidation and have been utilized in fuel cells and hydrogen storage.[25−28] In particular, AuPd bimetallic nanoparticles have become one of the most attractive systems in catalysis research due to its highly coordinative instauration on the surface.[29−33] In this work, the electrocatalysis of AuPd nanoparticles toward $NaBH_4$ oxidation was used to produce an electrochemical signal

Received: April 15, 2013
Accepted: June 3, 2013
Published: June 3, 2013

   dx.doi.org/10.1021/ac401105p | Anal. Chem. 2013, 85, 6505−6510

for immunoassay. The detection strategy used ADA-labeled antibody (ADA−Ab) to competitively bind the antigen immobilized on multiwalled carbon nanotube (MWCNT)-modified electrode surface and the target in solution, and the immobilized ADA then bound β-CD-functionalized AuPd nanoparticles (AuPd−CDs) to catalyze the oxidation of $NaBH_4$ on the electrode surface (Scheme 1). Using

Scheme 1. Preparation of (A) ADA−Ab Conjugate and (B) β-CD-Functionalized AuPd Bimetallic Nanoparticles, and (C) Electrochemical Immunoassay Procedure for the Detection of a Small Molecule

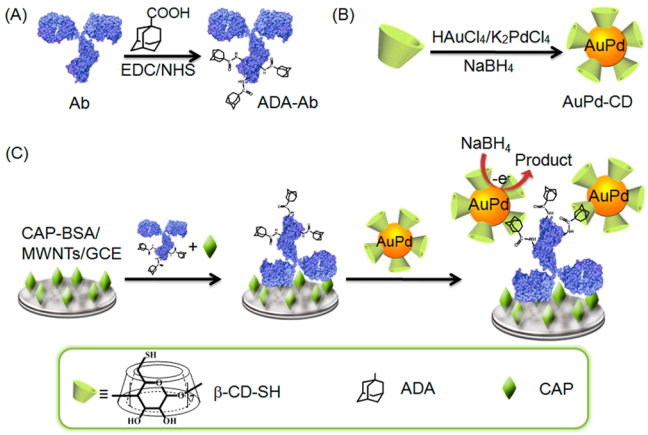

chloramphenicol (CAP, 323.13 Da),[34] a broad-spectrum antibiotic, as a model analyte, an ultrasensitive immunoassay method for CAP was developed. The proposed method showed a detection range of 6 orders of magnitude. The supramolecular host−guest interaction strategy provides a universal labeling approach for signal amplification and significantly demonstrates proof-of-concept for the detection of small molecules.

EXPERIMENTAL SECTION

Materials and Reagents. Chloramphenicol−bovine serum albumin (CAP−BSA) conjugate and chloramphenicol monoclonal antibody (Ab) were purchased from Shanghai Jieyi Biological Technology Ltd. (China). Chloroauric acid ($HAuCl_4{\cdot}4H_2O$), potassium chloropalladite (K_2PdCl_4), BSA, 1-ethyl-3-(3-(dimethylamino)propyl)carbodiimide hydrochloride (EDC), and *N*-hydroxysuccinimide (NHS) were purchased from Sigma-Aldrich Chemical Co. (St. Louis, MO). Chloramphenicol was purchased from Shanghai Sunshine Biotech Co., Ltd. (China). MWCNTs with a diameter of 40−60 nm were obtained from Shenzhen Nanotech Port Company (China). Mercapto-β-cyclodextrin (β-CD-SH) was purchased from Shandong Zhiyuan Biotechnology Ltd. (China). 1-Adamantanecarboxylic acid (99%) was purchased from Shanghai J&K Chemical Ltd. (China). Phosphate-buffered saline (PBS) was prepared by mixing the stock solutions of NaH_2PO_4 and Na_2HPO_4 (50 mM, pH 7.4). Borate buffer solutions (0.1 M) at pH 9.0, 10.0, 11.0, 12.0, and 12.7 were composed of H_3BO_3 and NaOH. Chloramphenicol Eye Drops was purchased from DiRui Pharmaceutic Co., Ltd. (Changchun, China) and used with dilution. All aqueous solutions were prepared using ultrapure water (≥18 MΩ, Milli-Q, Millipore).

Apparatus. To characterize the ADA−Ab conjugate, matrix-assisted laser desorption/ionization time-of-flight (MALDI-TOF) mass spectrometric experiments were performed using an Applied Biosystems 4800 proteomics analyzer (Applied Biosystems) equipped with a Nd:YAG laser operating at 355 nm, a repetition rate of 200 Hz, and an acceleration voltage of 20 kV. High resolution transmission electron microscopy (TEM) with energy dispersive X-ray analysis (EDX) was performed at 200 kV using a JEM-2100 TEM (JEOL, Japan). The X-ray photoelectron spectrum (XPS) was recorded with a PHI5000 VersaProbe X-ray photoelectron spectrometer (ULVAC-PHI Co. Japan). The ultraviolet−visible (UV−vis) spectra of CD-capped AuPd nanoparticles were obtained with a UV-3600 UV−vis−NIR spectrophotometer (Shimadzu, Japan). Linear sweep voltammetric (LSV) and cycling voltammetric (CV) measurements were performed using a CHI 630D electrochemical workstation (CH Instruments Inc., Austin, TX).

Preparation and Characterization of ADA−Ab Conjugate. A 33 mg amount of adamantanecarboxylic acid was suspended in 40 mL of water followed by adding 20 μL of 1 M NaOH to obtain a clear solution, which was immediately diluted to 100 mL. EDC (10 mg) and NHS (10 mg) were added to 2 mL of ADA solution and then mixed with 2 mL of PBS (50 mM, pH 7.4). After the mixture was gently shaken at room temperature for 30 min, 200 μL of CAP−Ab solution (1 mg/mL) was injected into this mixture and overnight at 4 °C. This solution was then concentrated by centrifugation (8000 rpm for 8 min) using a Microcon 10 kDa centrifugal filter device (from Milipore). The ADA−Ab conjugate was collected by inverting the Micro con filter, washing with 50 mM pH 7.4 PBS, and storing at −20 °C when not being used.

MALDI-TOF mass spectrometry was used to quantify the number of ADA molecules conjugated to each antibody. First, 1 mg/mL of ADA−Ab was dissolved in Milli-Q water using a 0.5 mL microconcentrator (Millipore Amicon; MWCO: 10KDa), and sinapinic acid (1 mg, Thermo Fisher Scientific) as a MALDI matrix was dissolved in a mixture of 70 μL acetonitrile (Sigma-Aldrich) and 30 μL water containing 0.1% trifluoroacetic acid (TFA, Sigma-Aldrich). The ADA−Ab solution (0.5 μL) was then deposited onto the MALDI plate and mixed with the MALDI matrix (0.5 μL) for mass spectrometric measurement.

Preparation of AuPd−CD Nanoparticles. The CD-capped AuPd nanoparticles were prepared according to the previous report with modifications.[35] First, all the glass materials were cleaned by treating with aqua regia. Afterward, in a typical synthesis of AuPd−CD nanoparticles, 20 mg $NaBH_4$ was added to 5 mL of aqueous solution of β-CD-SH, and then an aqueous solution of $HAuCl_4/K_2PdCl_4$ mixture in a molar ratio of 1:1 (0.4 mL, 5 mM) was injected with stirring. The solution changed from light yellow to deep brown immediately, indicative of nanoparticle formation. Next, this mixture was stirred overnight and then centrifuged at 8000*g* for 10 min using a 5 mL microconcentrator. The supernatant was discarded, and the sediment was rinsed twice with 5 mL of water. After centrifugation, the AuPd−CD nanoparticles were resuspended in 2 mL of water. This procedure produced a stable colloid solution of CD-capped AuPd nanoparticles with a diameter distribution of 3.2−4.2 nm, which could be stored at RT for more than 6 months without loss of activity.

Preparation of Immunosensor. MWNTs (100 mg) were first treated with 3:1 H_2SO_4/HNO_3 and sonicated for 4 h to obtain carboxylic group-functionalized MWCNTs for better dispersion. The resulting suspension was centrifuged, and the

dx.doi.org/10.1021/ac401105p | *Anal. Chem.* 2013, 85, 6505−6510

precipitate was washed thoroughly with water until the pH value was about 7.0. The black solid was collected and dried under vacuum at 80 °C. Then, the oxidized MWNTs were dispersed in water to a concentration of 0.5 mg/mL.[36]

The glassy carbon electrode (GCE, 3 mm diameter) was polished with 0.05 μm alumina slurry (Beuhler), followed by rinsing thoroughly with water. After successive sonication in water twice, the electrode was rinsed with water and dried by N_2 at RT. Five microliters of MWNT suspension (0.5 mg/mL) was then dropped on the pretreated GCE and dried at RT, which accelerated the electron transfer and enhanced the loading of CAP−BSA due to excellent conductivity and the high surface-to-volume ratio. Five microliters of CAP−BSA (1.0 mg/mL) was diluted to 0.5 mg/mL with 50 mM pH 7.4 PBS containing 1% BSA and then dropped on the MWCNT-coated electrode, which was then incubated in a water vapor-saturated environment at RT for 40 min to allow the passive adsorption of CAP−BSA on the electrode surface. The presence of BSA can block the nonspecific adsorption of other species in the immunoassay. After incubation, excess antigen was rinsed away with water, and the resulting immunosensor was stored at 4 °C prior to use.

Analytical Procedure. CAP solutions (10 μL) with different concentrations or samples were mixed with 10 μL of prepared ADA−Ab to obtain the incubation solutions. Sequentially, 5 μL of incubation solution was dropped on the CAP immunosensor and incubated for 40 min at 25 °C and then washed carefully with water, followed by incubation with 5 μL of AuPd−CD nanoparticle solution to obtain AuPd−CD/ADA−Ab/CAP−BSA/MWNTs/GCE. During the incubation process, the immunosensor was placed in a container to avoid the evaporation of incubation solution. The electrochemical measurement was performed in 0.1 M pH 11.0 H_3BO_3−NaOH in the presence of 5 mM $NaBH_4$ after incubation for 60 s to activate the catalytic activity of AuPd nanoparticles. The LSV measurements were from 600 to −300 mV at a scan rate of 50 mV/s. The data for condition optimization and the calibration curve were obtained with the average of three measurements.

RESULTS AND DISCUSSION

Cyclic Voltammetric Behavior of the Immunosensor. The electrocatalytic activity of the AuPd−CD nanoparticles toward $NaBH_4$ oxidation was first recorded with cyclic voltammograms. At the bare GCE, $NaBH_4$ did not show any detectable signal in 0.1 M pH 11.0 H_3BO_3−NaOH buffer in the examined potential range (Figure 1, curve a), while it showed two typical oxidation peaks at +0.15 V and +0.26 V corresponding to the oxidation of $NaBH_4$ and its intermediate at the AuPd−CD nanoparticle-modified electrode (Figure 1, curve c), which was obtained by the immunoreaction of ADA−Ab at the immunosensor and the following host−guest interaction with AuPd−CD nanoparticles. Moreover, the peak current increased with the increasing concentration of $NaBH_4$ (Figure 6C), indicating that the response came from the oxidation of $NaBH_4$ in the presence of AuPd−CD as catalyst. Because $NaBH_4$ undergoes multielectron (maximum $8e^-$) oxidation on Pd nanoparticles,[37,38] the current signal is much higher than those from the electrochemical reactions involving one-electron or two-electron oxidation. When the immunosensor was incubated directly with AuPd−CD nanoparticles in the absence of ADA−Ab, it showed only low background current (Figure 1, curve b), indicating negligible nonspecific absorption of AuPd−CD on the CAP−BSA-coated surface.

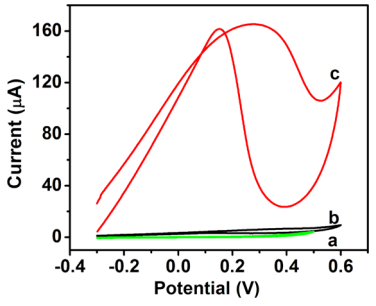

Figure 1. Cyclic voltammograms of bare GCE (a) and immunosensor incubated with AuPd−CD in the absence (b) and presence of ADA−Ab (c) in 0.1 M pH 11.0 H_3BO_3−NaOH buffer containing 5 mM $NaBH_4$. Scan rate: 50 mV/s.

Characterization of ADA−Ab Conjugate and AuPd−CD Nanoparticles. ADA−Ab was synthesized by conjugating EDC/NHS activated adamantanecarboxylic acid to CAP Ab that contains ∼90 amine groups.[39] From the mass spectra of CAP Ab and ADA−Ab (Figure 2A and 2B), the number of ADA moieties loaded on a single antibody was calculated to be ∼7, which provided a possibility for designing of a multilabel detection platform.

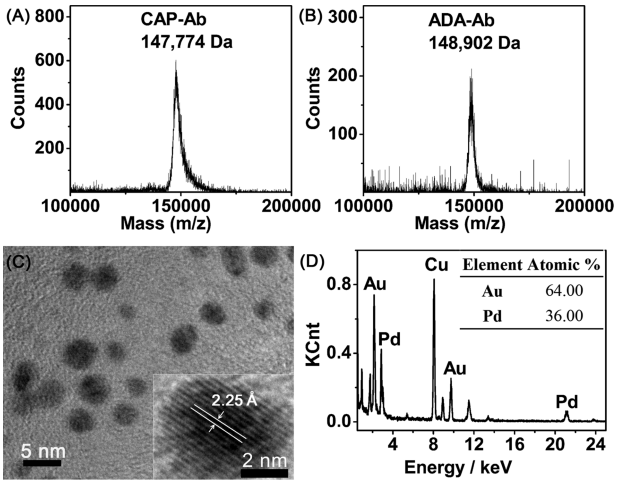

Figure 2. MALDI-TOF mass spectra of (A) CAP Ab and (B) ADA−Ab conjugate, (C) TEM image, and (D) EDX spectrum of AuPd−CD. Insets in C and D are the high-resolution TEM image and atomic ratio of Au/Pd, respectively.

On the basis of the interaction between Au/Pd and thiol, AuPd−CD nanoparticles were synthesized in aqueous solution instead of DMSO solution,[40] which can enhance the biocompatibility and electrocatalytic activity. The TEM image displayed a spherical shape of AuPd−CD nanoparticles and a size distribution ranging from 3.2 to 4.2 nm (Figure 2C). High-resolution TEM demonstrated that the *d* spacing for adjacent lattice fringes of the AuPd−CD nanoparticles was 2.25 Å (inset in Figure 2C), which corresponds to the (111) planes of the face-centered cubic crystalline structure. The energy-dispersive X-ray spectrum showed the signals of both Au and Pd, at a Au/Pd molar ratio of ∼2:1, which confirmed the formation of AuPd−CD nanoparticles (Figure 2D). In addition, the AuPd−CD dispersed in water showed a homogeneous solution (inset in Figure 3). Moreover, the absence of the surface plasmon

dx.doi.org/10.1021/ac401105p | Anal. Chem. 2013, 85, 6505−6510

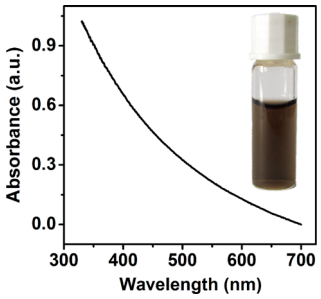

Figure 3. UV−vis spectrum of AuPd−CD nanoparticles in aqueous solution. Inset: photography of AuPd−CD nanoparticle solution.

peak of Au at 520 nm indicated that Au atoms were deposited only in a few areas across the surface of the AuPd bimetallic nanoparticles (Figure 3). These high-energy surfaces of AuPd−CD nanoparticles provide a potential route for enhancing the catalytic activity toward $NaBH_4$ oxidation.[41]

The XPS of Au4f, Pd3d, and S2p were recorded to further indentify the formation of the AuPd−CD nanoparticles (Figure 4). The binding energy of Pd3d5/2 shifted from 337 eV of Pd nanoparticles to 334.5 eV (Figure 4B). The lower binding energy indicated an improved electronic structure of Pd in AuPd−CD nanoparticles for enhancing the electrocatalytic activity toward $NaBH_4$ oxidation.

Condition Optimization for the Synthesis of AuPd−CD Nanoparticles. The effect of Au composition on the electrocatalytic activity was first examined. As shown in Figure 5A, the presence of Au composition led to an increase of the electrocatalytic peak current for $NaBH_4$ oxidation by 1.6 times, because Au was expected to donate one 6s electron to the d-band of Pd during the catalytic oxidation of $NaBH_4$.[42,43] In addition, the presence of Au in the nanoparticle improved the adsorption/desorption characteristics of Pd for hydrogen. Therefore, AuPd−CD nanoparticles showed catalytic activity toward $NaBH_4$ oxidation higher than that of Pd nanoparticles. Furthermore, the AuPd−CD nanoparticles obtained at 1:1 ratio of $AuCl_4^-$ to $PdCl_4^{2-}$ showed the maximum catalytic peak current (Figure 5B), Thus, the optimal molar ratio of $AuCl_4^-$ to $PdCl_4^{2-}$ was 1:1.

The reduction agent for the synthesis of AuPd−CD nanoparticles also greatly affected the catalytic activity. Generally $NaBH_4$, L-ascorbic acid and sodium citrate can be used in the preparation of metallic nanoparticles. Because citrate and L-ascorbic acid have the capacity for chemical reduction and have a coordination effect, they can be used as reducing and capping agents, which may affect the nanoparticle activity. Here $NaBH_4$ was used for synthesis of AuPd−CD nanoparticles to obtain the best electrocatalytic performance

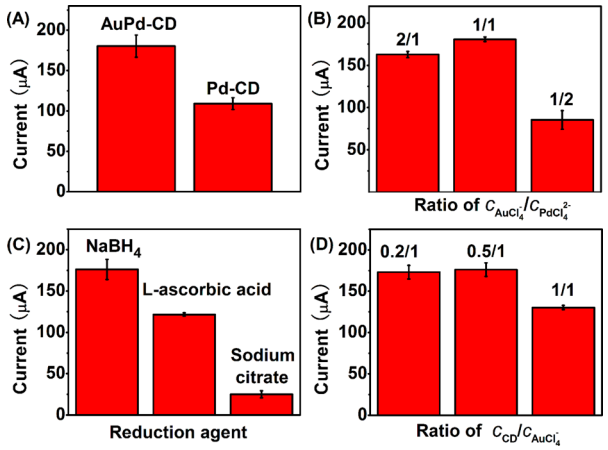

Figure 5. Effects of (A) compositions, (B) concentration ratio of $AuCl_4^-/PdCl_4^{2-}$, (C) reduction agents, and (D) concentration ratio of $CD/AuCl_4^-$ for synthesis of AuPd−CD nanoparticles on catalytic peak current of the immunosensor toward $NaBH_4$ oxidation.

(Figure 5C), which should contribute to the strong reduction properties of $NaBH_4$ and the formation of Pd−H during the reduction of $AuCl_4^-$ and $PdCl_4^{2-}$.[44]

The effect of the CD concentration on the electrocatalytic activity was investigated in Figure 5D. The AuPd−CD nanoparticles prepared at a 0.5 ratio of CD to $AuCl_4^-$ showed the largest response, because the growth of AuPd−CD nanoparticles depended on the dynamic attachment of the thiolated CD to the surface of the AuPd nanoparticles.

Optimization of Conditions for Electrochemical Immunoassay. To provide sufficient recognition sites for ADA−Ab, the concentration of CAP−BSA for immunosensor preparation was optimized. The peak current increased with the increasing CAP−BSA concentration up to 0.5 mg/mL (Figure 6A). Therefore, 0.5 mg/mL CAP−BSA was chosen. The incubation time and concentration of AuPd−CD nanoparticles for host−guest interaction were also optimized to be 40 min (Figure 6B) and 303.4 μg/mL (Figure S1 in Supporting Information) for obtaining high sensitivity.

The concentration of $NaBH_4$ and pH of borate buffer were investigated in the following experiments. As shown in Figure 6C and 6D, the optimal conditions were 5 mM and 11.0, respectively.

Electrochemical Response to CAP. Under optimized conditions, a competitive immunoassay configuration was performed by mixing CAP at a known concentration into the incubation solution containing ADA−Ab. The CAP in the incubation solution competed with the CAP immobilized on the immunosensor surface to bind the limited binding sites of

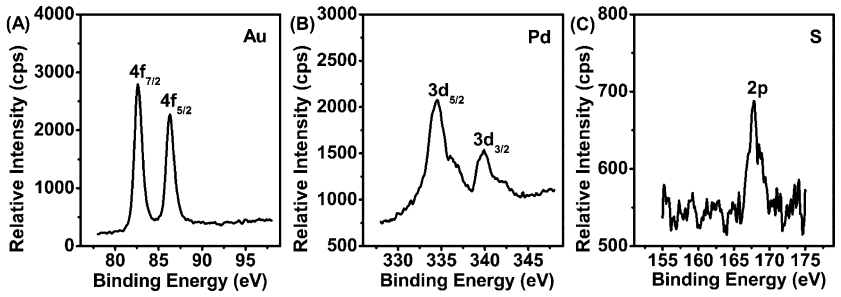

Figure 4. XPS spectra of (A) Au 4f, (B) Pd 3d, and (C) S2p for AuPd−CD nanoparticles.

dx.doi.org/10.1021/ac401105p | Anal. Chem. 2013, 85, 6505−6510

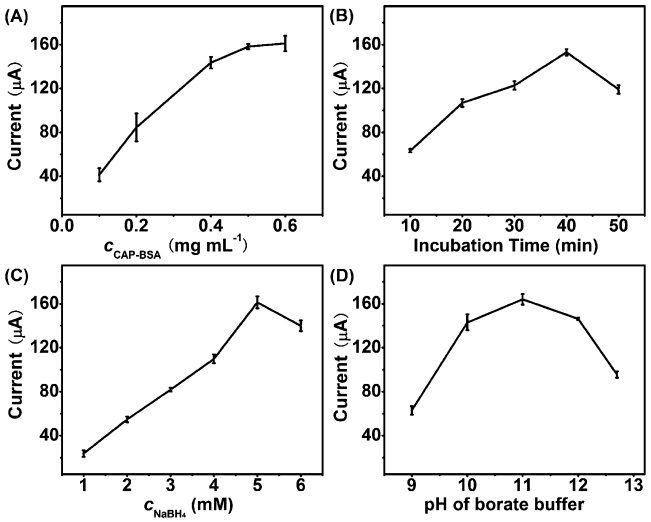

Figure 6. Effects of (A) CAP–BSA concentration for immunosensor preparation, (B) incubation time for AuPd–CD nanoparticles, (C) $NaBH_4$ concentration, and (D) pH of borate buffer for immunoassay upon initial immunosensor response.

ADA–Ab to form the immunocomplex. The captured ADA–Ab on the immunosensor surface further bound AuPd–CD through host–guest interaction, which was confirmed by a TEM image showing a 3–6 AuPd nanoparticle aggregation (Figure S2, Supporting Information). The aggregated AuPd nanoparticles catalyzed the oxidation of $NaBH_4$ to produce the detectable signal. As shown in Figure 7A, the peak current

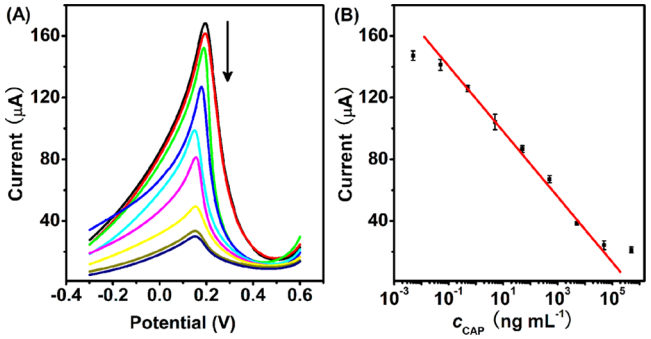

Figure 7. (A) LSV responses and (B) calibration curve of the CAP immunosensor in 0.1 M borate buffer (pH 11) containing 5 mM $NaBH_4$ after incubation with CAP ranging from 5×10^{-3} to 5×10^{5} ng/mL (from top to bottom). Scan rate: 50 mV/s.

decreased with increasing CAP concentration in the incubation solution. The decrease of peak current was proportional to CAP concentration in the range of 50 pg/mL to 50 μg/mL with a correlation coefficient of 0.996 (Figure 7B). The detectable concentration range was much wider than 0.1–1000 ng/mL for a label-free electrochemical immunosensor[45] and 0.5–100 ng/mL for a piezoelectric immunosensor.[46] The detection limit was calculated to be 4.6 pg/mL at a signal-to-noise ratio of 3, which was much lower than 10 ng/mL for immunochromatographic assay,[47] 0.65 ng/mL for a molecularly imprinted polymer-based voltammetric sensor,[48] and 0.3 ng/mL of the minimum required performance level set up by EU in food safety.[49] Thus, the proposed method was acceptable for practical application.

Precision, Stability, and Sample Detection. The intra-assay variation coefficients of this method with five immunosensors were 3.4% and 2.9% at a CAP concentration of 0.5 and 5 μg/mL, respectively, indicating acceptable precision and fabrication reproducibility. When the immunosensor was not in use, it was stored at 4 °C. A 93.5% initial response from the immunosensor for CAP was retained after one week. This result indicated that the immunosensor had acceptable stability.

The analytical reliability and application potential of the proposed method was evaluated by the analysis of the CAP Eye Drops sample. The CAP concentration determined with this method was 12.7 ± 0.2 μg/mL, which was consistent with the referred value of 12.5 μg/mL, indicating that ethylmercurithiosalicylic acid as an additive in CAP Eye Drops did not interfere with the detection. Thus, the present method satisfied the need for the detection of CAP in practice.

CONCLUSIONS

A universal immunoassay platform was designed for ultrasensitive electrochemical detection of small molecules by host–guest interaction using AuPd bimetallic nanoparticles as a signal tag. Because of the small size of ADA and the steric advantages, a large amount of ADA-labeled antibody was bound to the immunosensor surface to capture AuPd–CD nanoparticles for realizing a wide detection range for the competitive immunoassay. The small size of ADA allowed more ADA to be bound to a single antibody to achieve multiple labels for the binding event, which amplified the detectable signal and thus improved the sensitivity of competitive immunoassay. Because $NaBH_4$ undergoes multielectron oxidation on AuPd nanoparticles, the sensitivity could be further enhanced. The proposed immunosensing method for detection of CAP showed a wide linear range, low detection limit, and acceptable precision and stability, indicating promising application for the analysis of small molecule targets.

ASSOCIATED CONTENT

Supporting Information

Additional information as noted in the text. This material is available free of charge via the Internet at http://pubs.acs.org.

AUTHOR INFORMATION

Corresponding Author

*Phone/Fax: +86-25-83593593. E-mail: jpl@nju.edu.cn; hxju@nju.edu.cn.

Notes

The authors declare no competing financial interest.

ACKNOWLEDGMENTS

This work was financially supported by the National Basic Research Program of China (2010CB732400), National Natural Science Foundation of China (21075060, 21135002, 21121091), and Excellent Talents in Chinese Universities (NCET100479).

REFERENCES

(1) Quinton, J.; Kolodych, S.; Chaumonet, M.; Bevilacqua, V.; Nevers, M. C.; Volland, H.; Gabillet, S.; Thuéry, P.; Créminon, C.; Taran, F. *Angew. Chem., Int. Ed.* **2012**, *51*, 6144–6148.

(2) Qu, W. S.; Liu, Y. Y.; Liu, D. B.; Wang, Z.; Jiang, X. Y. *Angew. Chem., Int. Ed.* **2011**, *50*, 3442–3445.

(3) Krishnan, S.; Mani, V.; Wasalathanthri, D.; Kumar, C. V.; Rusling, J. F. *Angew. Chem., Int. Ed.* **2011**, *50*, 1175−1178.
(4) Munge, B. S.; Coffey, A. L.; Doucette, J. M.; Somba, B. K.; Malhotra, R.; Patel, V.; Gutkind, J. S.; Rusling, J. F. *Angew. Chem., Int. Ed.* **2011**, *50*, 7915−7918.
(5) Das, J.; Aziz, M. A.; Yang, H. *J. Am. Chem. Soc.* **2006**, *128*, 16022−16023.
(6) de La Rica, R.; Stevens, M. M. *Nat. Nanotechnol.* **2012**, *7*, 821−824.
(7) Wei, Q.; Zhao, Y. F.; Du, B.; Wu, D.; Cai, Y. Y.; Mao, K. X.; Li, H.; Xu, C. X. *Adv. Funct. Mater.* **2011**, *21*, 4193−4198.
(8) Date, Y.; Aota, A.; Terakado, S.; Sasaki, K.; Matsumoto, N.; Watanabe, Y.; Matsue, T.; Ohmura, N. *Anal. Chem.* **2012**, *85*, 434−440.
(9) Lai, L. M. H.; Goon, I. Y.; Chuah, K.; Lim, M.; Braet, F.; Amal, R.; Gooding, J. J. *Angew. Chem., Int. Ed.* **2012**, *51*, 6456−6459.
(10) Orlov, A. V.; Khodakova, J. A.; Nikitin, M. P.; Shepelyakovskaya, A. O.; Brovko, F. A.; Laman, A. G.; Grishin, E. V.; Nikitin, P. I. *Anal. Chem.* **2013**, *85*, 1154−1163.
(11) Zhang, J.; Lei, J. P.; Xu, C. L.; Ding, L.; Ju, H. X. *Anal. Chem.* **2010**, *82*, 1117−1122.
(12) Tan, W. M.; Huang, Y.; Nan, T. G.; Xue, C. G.; Li, Z. H.; Zhang, Q. C.; Wang, B. M. *Anal. Chem.* **2010**, *82*, 615−620.
(13) Cella, L. N.; Chen, W.; Myung, N. V.; Mulchandani, A. *J. Am. Chem. Soc.* **2010**, *132*, 5024−5026.
(14) Wang, H.; Wang, S. T.; Su, H.; Chen, K. J.; Armijo, A. L.; Lin, W. Y.; Wang, Y. J.; Sun, J.; Kamei, K. I.; Czernin, J.; Radu, C. G.; Tseng, H. R. *Angew. Chem., Int. Ed.* **2009**, *48*, 4344−4348.
(15) Tao, W.; Liu, Y.; Jiang, B. B.; Yu, S. R.; Huang, W.; Zhou, Y. F.; Yan, D. Y. *J. Am. Chem. Soc.* **2012**, *134*, 762−764.
(16) Uhlenheuer, D. A.; Petkau, K.; Brunsveld, L. *Chem. Soc. Rev.* **2010**, *39*, 2817−2826.
(17) Hennig, A.; Bakirci, H.; Nau, W. M. *Nat. Methods* **2007**, *4*, 629−632.
(18) Kim, C.; Agasti, S. S.; Zhu, Z. J.; Isaacs, L.; Rotello, V. M. *Nat. Chem.* **2010**, *2*, 962−966.
(19) Zhao, Y. L.; Li, Z. X.; Kabehie, S.; Botros, Y. Y.; Stoddart, J. F.; Zink, J. I. *J. Am. Chem. Soc.* **2010**, *132*, 13016−13025.
(20) Escalante, M.; Zhao, Y. P.; Ludden, M. J. W.; Vermeij, R.; Olsen, J. D.; Berenschot, E.; Hunter, C. N.; Huskens, J.; Subramaniam, V.; Otto, C. *J. Am. Chem. Soc.* **2008**, *130*, 8892−8893.
(21) Lee, D. W.; Park, K. M.; Banerjee, M.; Ha, S. H.; Lee, T.; Suh, K.; Paul, S.; Jung, H.; Kim, J.; Selvapalam, N.; Ryu, S. H.; Kim, K. *Nat. Chem.* **2011**, *3*, 154−159.
(22) Chinai, J. M.; Taylor, A. B.; Ryno, L. M.; Hargreaves, N. D.; Morris, C. A.; Hart, P. J.; Urbach, A. R. *J. Am. Chem. Soc.* **2011**, *133*, 8810−8813.
(23) de La Rica, R.; Fratila, R. M.; Szarpak, A.; Huskens, J.; Velders, A. H. *Angew. Chem., Int. Ed.* **2011**, *50*, 5704−5707.
(24) Agasti, S. S.; Liong, M.; Tassa, C.; Chung, H. J.; Shaw, S. Y.; Lee, H.; Weissleder, R. *Angew. Chem., Int. Ed.* **2012**, *51*, 450−454.
(25) Lim, B.; Jiang, M. J.; Camargo, P. H. C.; Cho, E. C.; Tao, J.; Lu, X. M.; Zhu, Y. M.; Xia, Y. N. *Science* **2009**, *324*, 1302−1305.
(26) Kobayashi, H.; Yamauchi, M.; Kitagawa, H.; Kubota, Y.; Kato, K.; Takata, M. *J. Am. Chem. Soc.* **2008**, *130*, 1818−1819.
(27) Das, J.; Kim, H.; Jo, K.; Park, K. H.; Jon, S.; Lee, K.; Yang, H. *Chem. Commun.* **2009**, 6394−6396.
(28) Tappan, B. C.; Steiner, S. A.; Luther, E. P. *Angew. Chem., Int. Ed.* **2010**, *49*, 4544−4565.
(29) Zhang, H. J.; Watanabe, T.; Okumura, M.; Haruta, M.; Toshima, N. *Nat. Mater.* **2012**, *11*, 49−52.
(30) Kim, D.; Lee, Y. W.; Lee, S. B.; Han, S. W. *Angew. Chem., Int. Ed.* **2012**, *51*, 159−163.
(31) Ding, Y.; Fan, F. R.; Tian, Z. Q.; Wang, Z. L. *J. Am. Chem. Soc.* **2010**, *132*, 12480−12486.
(32) Henning, A. M.; Watt, J.; Miedziak, P. J.; Cheong, S.; Santonastaso, M.; Song, M. H.; Takeda, Y.; Kirkland, A. I.; Taylor, S. H.; Tilley, R. D. *Angew. Chem., Int. Ed.* **2013**, *52*, 1477−1480.
(33) Hong, J. W.; Kim, D.; Lee, Y. W.; Kim, M.; Kang, S. W.; Han, S. W. *Angew. Chem., Int. Ed.* **2011**, *50*, 8876−8880.
(34) Allen, E. H. *J. Assoc. Off. Anal. Chem.* **1985**, *68*, 990−999.
(35) Liu, J.; Mendoza, S.; Román, E.; Lynn, M. J.; Xu, R. L.; Kaifer, A. E. *J. Am. Chem. Soc.* **1999**, *121*, 4304−4305.
(36) Lai, G. S.; Yan, F.; Ju, H. X. *Anal. Chem.* **2009**, *81*, 9730−9736.
(37) de Leon, C. P.; Walsh, F. C.; Pletcher, D.; Browning, D. J.; Lakeman, J. B. *J. Power Sources* **2006**, *155*, 172−181.
(38) Simões, M.; Baranton, S.; Coutanceau, C. *J. Phys. Chem. C* **2009**, *113*, 13369−13376.
(39) Haun, J. B.; Devaraj, N. K.; Hilderbrand, S. A.; Lee, H.; Weissleder, R. *Nat. Nanotechnol.* **2010**, *5*, 660−665.
(40) Liu, J.; Ong, W.; Román, E.; Lynn, M. J.; Kaifer, A. E. *Langmuir* **2000**, *16*, 3000−3002.
(41) Tian, N.; Zhou, Z. Y.; Sun, S. G.; Ding, Y.; Wang, Z. L. *Science* **2007**, *316*, 732−735.
(42) Chatenet, M.; Micoud, F.; Roche, I.; Chainet, E. *Electrochim. Acta* **2006**, *51*, 5459−5467.
(43) Zhang, J.; Sasaki, K.; Sutter, E.; Adzic, R. R. *Science* **2007**, *315*, 220−222.
(44) Narehood, D. G.; Kishore, S.; Goto, H.; Adair, J. H.; Nelson, J. A.; Gutiérrez, H. R.; Eklund, P. C. *Int. J. Hydrogen Energy* **2009**, *34*, 952−960.
(45) Zhang, N. D.; Xiao, F.; Bai, J.; Lai, Y. J.; Hou, J.; Xian, Y. Z.; Jin, L. T. *Talanta* **2011**, *87*, 100−105.
(46) Karaseva, N. A.; Ermolaeva, T. N. *Talanta* **2012**, *93*, 44−48.
(47) Byzova, N. A.; Zvereva, E. A.; Zherdev, A. V.; Eremin, S. A.; Dzantiev, B. B. *Talanta* **2010**, *81*, 843−848.
(48) Alizadeh, T.; Ganjali, M. R.; Zare, M.; Norouzi, P. *Food Chem.* **2012**, *130*, 1108−1114.
(49) Commission Decision, 2003/181/ED of 13 March 2003. *Off. J. Eur. Commun.* **2003**, *L71*, 17−18.